Systemic and strict regulation of the glutathione redox state in mitochondria and cytosol is needed for zebrafish ontogeny

Kristin Hamre, Wuxiao Zhang, Maren Hoff Austgulen, Eva Mykkeltvedt, Peng Yin, Marc Berntssen, Marit Espe, Carsten Berndt

Suggested Citation:
Hamre, K., Zhang, W., Austgulen, M. H., Mykkeltvedt, E., Yin, P., Berntssen, M., Espe, M., & Berndt, C. (2024). Systemic and strict regulation of the glutathione redox state in mitochondria and cytosol is needed for zebrafish ontogeny. Biochimica et Biophysica Acta: BBA, 1868(6), Article 130603. https://doi.org/10.1016/j.bbagen.2024.130603

BBA - General Subjects 1868 (2024) 130603

Contents lists available at ScienceDirect

BBA - General Subjects

journal homepage: www.elsevier.com/locate/bbagen

Systemic and strict regulation of the glutathione redox state in mitochondria and cytosol is needed for zebrafish ontogeny

Kristin Hamre [a,d,*], Wuxiao Zhang [a,c], Maren Hoff Austgulen [a], Eva Mykkeltvedt [a], Peng Yin [a,1], Marc Berntssen [a], Marit Espe [a], Carsten Berndt [b,**]

[a] Department of Feed and Nutrition, The Institute of Marine Research, Bergen, Norway
[b] Department of Neurology, Medical Faculty, Heinrich-Heine-Universitaet, Duesseldorf, Germany
[c] College of Marine and Biology Engineering, Yancheng Institute of Technology, Yancheng 224051, China
[d] Hamre Aquatic Nutrition, Breiviken 8, 5042 Bergen, Norway

ARTICLE INFO

Keywords:
roGFP probe
Zebrafish model
Embryonic development
Glutathione metabolism
PFOS

ABSTRACT

Background: Redox control seems to be indispensable for proper embryonic development. The ratio between glutathione (GSH) and its oxidized disulfide (GSSG) is the most abundant cellular redox circuit.
Methods: We used zebrafish harboring the glutaredoxin 1-redox sensitive green fluorescent protein (Grx1-roGFP) probe either in mitochondria or cytosol to test the hypothesis that the GSH:GSSG ratio is strictly regulated through zebrafish embryogenesis to sustain the different developmental processes of the embryo.
Results: Following the GSSG:GSH ratio as a proxy for the GSH-dependent reduction potential (E_{hGSH}) revealed increasing mitochondrial and cytosolic E_{hGSH} during cleavage and gastrulation. During organogenesis, cytosolic E_{hGSH} decreased, while that of mitochondria remained high. The similarity between E_{hGSH} in brain and muscle suggests a central regulation. Modulation of GSH metabolism had only modest effects on the GSSG:GSH ratios of newly hatched larvae. However, inhibition of GSH reductase directly after fertilization led to dead embryos already 10 h later. Exposure to the emerging environmental pollutant Perfluorooctane Sulfonate (PFOS) disturbed the apparent regulated E_{hGSH} as well.
Conclusions: Mitochondrial and cytosolic GSSG:GSH ratios are almost identical in different organs during zebrafish development indicating that the E_{hGSH} might follow H_2O_2 levels and rather indirectly affect specific enzymatic activities needed for proper embryogenesis.
General significance: Our data confirm that vertebrate embryogenesis depends on strictly regulated redox homeostasis. Disturbance of the GSSG:GSH circuit, e.g. induced by environmental pollution, leads to malformation and death.

1. Introduction

Oxidative distress is a pathophysiological situation causing disturbed redox signaling and cellular damage, whereas oxidative eustress establishes the redox homeostasis of organelles to regulate metabolism [1,2] and is indispensable for various processes including embryonic development [3–5]. Hydrogen peroxide (H_2O_2) is the major oxidizing second messenger with an intracellular concentration range between 10 and 1000 nM [6]. Glutathione (GSH) scavenges H_2O_2 and is oxidized to glutathione disulfide (GSSG). GSSG is reduced back by NADPH-dependent GSH reductase (GR). Although not a single biological function is described as solely GSH-dependent so far, GSH is an important cofactor for several enzymes and regulates enzymatic activity via post-translational modifications of redox switches and thereby the direction of metabolism [6–8]. The GSH/GSSG couple is the most abundant redox buffer, but reversibility of thiol redox switches is mostly guaranteed by

Abbreviations: BSO, Buthionine sulphoximine; E_{hGSH}, GSH-dependent reduction potential; GSH, glutathione; GSSG, glutathione disulfide; hpf, hours post fertilization; NAC, *N*-acetyl-cysteine; PFOS, Perfluorooctane Sulfonate.

* Correspondence to: Hamre Aquatic Nutrition, Breiviken 8, 5042 Bergen, Norway.
** Correspondence to: Carsten Berndt, University Clinic and Medical Faculty, Heinrich-Heine University, Moorenstr, 5, Düsseldorf 40225, Germany.
E-mail addresses: post@kristinhamre.no (K. Hamre), berndt@hhu.de (C. Berndt).
[1] Present address: Institute of Animal Science, Guangdong Academy of Agricultural Sciences, Guangzhou 510640, China.

https://doi.org/10.1016/j.bbagen.2024.130603
Received 7 November 2023; Received in revised form 22 February 2024; Accepted 18 March 2024
Available online 21 March 2024

thioredoxins and glutaredoxins [9,10]. The GSH-dependent reduction potential (E_{hGSH}) for all tissues and cell compartments is in the range of −350 to −150 mV [11,12]. In zebrafish, an established model for (redox-dependent) vertebrate development [13,14] the E_{hGSH} ranges between −230 mV at fertilization and hatching to approximately −175 mV at gastrulation [15,16]. The total GSH (GSH^T) increased from fertilization until 30 hpf and was then stable until hatching allowing enzymatic activities of GSH-dependent proteins such as glutaredoxins that are essential for the formation of the nervous and vascular systems during zebrafish development [17–19]. In cod larvae the concentration of GSSG increased around the growth burst between 20 and 40 days after first-feeding that happens in well-nourished larvae [20], indicating that high growth rates and related metabolic changes coincide with more oxidized tissues. This was confirmed in Atlantic salmon that developed oxidized tissues and cataract during growth-stimulation in spring, when photoperiod and temperature increase [21,22]. It was also shown that tissues of Atlantic salmon implanted with growth hormone became more oxidized [23]. On the other hand, the E_{hGSH} of Atlantic salmon in a steady grow-out period did not differ during several months upon diets with wide variations of pro-and antioxidant nutrients at constant environmental conditions [24]. In the embryo, which develops from one cell to an organism with multiple events on the way, orchestration is necessary and redox signaling plays an important part in the organization of events in embryogenesis. Beside GSH and other molecules, this includes highly dynamic H_2O_2 levels, which have been monitored during zebrafish development using the genetically encoded probe HyPer [25,26].

In this study, we used two transgenic zebrafish lines with the glutaredoxin1-redox sensitive green fluorescent protein (Grx1-roGFP) probe implanted either in mitochondria (mito-line) or cytosol (cyto-line) [27]. This second generation ratiometric probe undergoes conformational changes dependent on the redox state of the coupled Grx1 leading to a change in absorbance at 510–525 nm after excitation at 405 or 488 nm [28].

Using this tool, we investigated the hypothesis that E_{hGSH} is strictly regulated in organelles through embryogenesis of zebrafish, to sustain the different developmental processes via promoting (in-)activation of metabolic redox switches. We followed the GSSG:GSH ratio during development and in addition the embryos were subjected to several modulators of glutathione metabolism and the environmental pollutant perfluorooctane sulfonate (PFOS), which is known to induce oxidative damage in zebrafish larvae [29].

2. Materials and methods

2.1. Ethical statement

The experiments complied with the guidelines of the Norwegian Regulation on Animal Experimentation and European Community Directive 86/609/EEC. The zebrafish facility of IMR has approval to work with transgene organisms according to the Regulation of 21.12.2001 no 1602. The approval was given by the Norwegian Ministry of Health 03.07.19.

2.2. Origin of zebrafish lines

The zebrafish lines expressing redox sensitive green fluorescent protein either in mitochondria (Tg:actin-mroGFP) or cytosol (Tg_actin-croGFP), were obtained from Karolinska Institutet and constructed as described in Bräutigam et al. [27].

2.3. Rearing and mating of F0 zebrafish and incubation of F(1-n) from fertilization until exogenous feeding

New generations of both lines of roGFP transgene zebrafish were made 1–2 times a year and the fish were ready for mating at approximately 3 months after hatching.

Zebrafish were held in a ZebTec Active Blue - Stand Alone system (Techniplast, Italy) at a temperature of 28.5 °C, conductivity 550 μS and pH 7.5. These parameters were monitored continuously. NH_3/NH_4, NO_2 and NO_3 were measured weekly to monitor biofilter function. The light regime was set at 14 h light and 10 h dark and the tank sizes used were 1.1, 3.5 and 8 L. The maximum density was 80 larvae, 15 adult fish or 40 adult fish per tank, respectively. The fish were fed the Gemma micro formulated diet (Skretting, Stavanger, Norway) three times a day at 08–10:00, 11:30–13:00 and 14–16:00 at a total of 3% biomass. The water treatment system (TYP ZERO 2000F (2015), Callidus, Sweeden) consisted of a cartridge filter (Cartucc A 20`` PA 5 MIC) a carbon filter (Harmsco HAC-BB-20-W, 10 μm) and a reverse osmosis unit (Axeon, model HF4–2540, Klart vann, Sandnes, Norway). System software by Tecniplast was used for continuous monitoring of water parameters.

Parental fish were separated by sex one week before mating and feeding was increased to approximately 5% of biomass to provide more nutrients for egg production. A total of 48 fish were separated for group matings with a ratio of 4 females to 2 males, placed in 1.7-L breeding tanks (Tecniplast, Italy) after final feeding. The following morning the water was exchanged, and the dividing wall was removed allowing for spawning for approximately 1 h. Fertilized embryos were incubated (Constant climate chamber HPP400, AtmoSAFE Memmert, Heidelberg Germany, 28.5 °C) in E3 embryo medium (stock solution: 17.2 g NaCl, 4.9 g $MgSO_4$*$7H_2O$, 2.9 g $CaCl_2$*$2H_2O$, 0.76 g KCl + 1 L dH_2O, used solution: 16.5 mL L^{-1} RO-water). The number of dishes corresponded to what was needed in the different experiments. For the ontogeny experiments, the density was 50 embryos / petridish, whereas the incubation experiments were performed with 20 embryo/petri dish (9 cm). At 1 dpf dead embryos were removed and fresh E3 medium was added to all dishes. After approximately 2 dpf in the incubation experiments, the embryos hatched naturally, and 10 larvae were transferred to 10 mL of E3 embryo medium for incubation with different chemicals (see below).

2.4. Development stages

Ontogeny of the zebrafish embryo is described by Kimmel et al. [30] (Table 1) and can grossly be divided into the following stages; zygote (1 cell), cleavage (2–128 cells), blastula 128 cells to 50% epiboly), gastrula (50% epiboly-somitogenesis). Somitogenesis, pharyngula, and hatching periods belong to the period of differentiation and organogenesis which continues through hatching. The period from zygote to the gastrula

Table 1
Sampling at developmental stages/time points (hours post fertilization hpf) in embryos held at 28.5 °C, as described by Kimmel (1995) with indication of measured tissues.

Sample no	Stage	Hpf	Cells/tissue measured
	Fertilization	0	
1	2 cell/fertilization	0,75	cells
2	Blastula 256 stage	2,50	cells
3	Blastusla MBT	2,75	cells
4	Blastula Dome stage - before epiboly	4,3	cells
5	Gastrula 50% epiboly	5,25	cells
6	Gastrula Bud stage (100% epiboly)	10	Trunk, neural plate, tail*
7	Segmentation four somite stage	11,3	Somite, neural plate, tail*
8	Period of enhanced lengthening (tail morphogenesis)	25	Somite, midbrain, tail*
9	Myotomes from first 3 somites	30	Myotomes, midbrain, tail*
10	Before hatching	48	Myotomes, midbrain, tail*
11	After hatching	50	Myotomes, midbrain, tail*

* Tail measured in cyto-line only.

stage takes 10.33 h at 28.5 °C, while organogenesis starts at the end of gastrulation. The embryos hatch at 48–72 h post fertilization (hpf).

2.5. Confocal microscopy

The larvae were immobilized in 200 mg/L MS-222 (Scan Aqua, Årnes, Norway), before they were placed in a glass bottomed petridish suitable for confocal microscopy (3–4 larvae per dish). They were mounted in three drops of 0,1% low melt agarose (A4018, Sigma Aldrich, St. Louis, MO, USA) in E3, containing 200 mg/L MS-222. After solidification, 3 mL of medium with chemical in the case of exposure experiments, was added to prevent the gel from drying out during microscopy. The larvae were photographed at 405 and 488 nm using a 3 step Z stack with a 20 μm range on a Nikon Eclipse Ti confocal microscope. The reduction potential was measured as the ratio of emission at 510 nm when the sample was excited at 405 or 488 nm. Different areas in the cell disc or embryo/larva organ had different intensities, but the ratio 405/488 was not affected by the intensity and measuring area. Nevertheless, a standardized measuring area and depth of the z-stack were used.

To check that the embryos were in good condition and responding to oxidative and reductive conditions, the 405/488 ratio in muscle of three newly hatched zebrafish mito- and cyto-line larvae held in E3 medium, was measured during 60 min while placed under the microscope. The 405/488 ratio of the fish stayed stable for this period of time (Fig. S1).

To follow time- and concentration-dependent activity of the probe, 40 mM of DTT or H_2O_2 or 0–100/500 mM of DTT or H_2O_2 were added to triplicate dishes 20 mins after the larvae were placed under the microscope and the 405/488 ratios were measured 20 mins after addition or for 60 mins (Fig. S1).

2.6. Generation of ratiometric pictures using ImageJ

A threshold was set for every pair of pictures taken at 405 and 488 nm and the background was removed. The intensity at 405 nm was divided by the intensity at 488 nm and the ratio is shown by the LTU fire as previously described by Fujikawa et al. [31].

2.7. Ontogeny of 405/488 ratio in mitochondria and cytosol of zebrafish embryo and yolk sac larvae

Zebrafish embryos were held under the conditions described above and sampled for Confocal microscopy at the stages given in Table 1 [30]. From the two-cell stage (2 hpf) until 50% epiboly (5.25 hpf) the 405/488 ratio was measured only in the cell disc. Depending on the developmental stage from 100% epiboly (10 hpf) until after hatching (50 hpf) the 405/488 ratio was measured in the trunk/ 4th somite/ 4th myotome (muscle), the neural plate/ midbrain (brain), and in in the cyto-line, only, the tail region. The embryos and larvae were immobilized as described above and subjected to microscopy. Four larvae were measured per developmental stage and the experiment was repeated three times.

2.8. Determination of GSH and GSSG

Zebrafish were spawned and the embryos incubated in 12 × 2 petridishes for the mito and cyto-line, respectively. Embryos from 3 dishes for each line were collected at 0, 11, 30 and 48 hpf and analyzed for GSH:GSSG using a commercial kit (Prod. No. GT40, Oxford Biomedical Research, Oxford, UK).

2.9. Incubation of zebrafish embryos and yolk sac larvae with modulators of glutathione metabolism and with the contaminant Perfluorooctane Sulfonate (PFOS)

Modulators of GSH metabolism used for the incubations were:

200 μM Carmustine/BCNU (C0400 Sigma Aldrich, St. Louis, MO, USA), an inhibitor of glutathione reductase (GR), 250 μM *N*-acetyl-L-cysteine (NAC, A9165, Sigma Aldrich, St. Louis, MO, USA), a precursor of cysteine which stimulates GSH synthesis, 15 μM L-Buthionine-(*S*,*R*)-sulfoximine (BSO, BML-FR117–0500, Enzo Life Sciences, Ann Harbour, MI, USA), an inhibitor of GSH synthesis, 40 μM trans-polydatin (PHL89312, Sigma Aldrich, St. Louis, MO, USA), an inhibitor of the pentose phosphate cycle which delivers NADPH for reduction reactions. We found that the chorion had low permeability to some of the chemicals, de-coronated embryos did not perform well in our hands. Newly hatched larvae were therefore used for most of these experiments, except carmustine, for which the chorion was permeable at the 2-cell stage. Embryos from both the cyto- and the mito-lines were first incubated until after hatching (50 hpf) under standard conditions, in triplicate petridishes for each chemical. The chemicals were then added, and larvae were incubated further until 74 hpf (24 h), 3 larvae per Petridish were immobilized and the 405/488 ratio was measured by confocal microscopy. Larvae in three Petridishes without addition of chemicals served as control.

In another experiment, newly hatched larvae (50 hpf) were incubated with 16, 32 and 64 μM PFOS (77,282, Sigma Aldrich, St. Louis, MO, USA) in triplicate until 74 hpf and then subjected to confocal microscopy, using the same procedures as for GSH modulators. Since PFOS is lipid soluble and had to be solubilized in DMSO (D8418, Sigma Aldrich, St. Louis, MO, USA) [32], the control in this experiment was added 0,01%DMSO, the same as the PFOS treatments.

For the carmustine experiments, newly fertilized embryos were incubated for 1–2, 6 and 10 h, in pertidishes with E3 embryo medium added carmustine to 200 μM. The carmustine stock solution was freshly prepared for each experiment. Eighteen petridishes were used, three for the carmustine treatment and three for the control at each sampling point. The petridishes with embryos were photographed and later the number of normal, deformed (arrest of cell division and development) and dead embryos were counted. Minimum three embryos ($n = 9$–16 per treatment) from each dish were taken for confocal microscopy, by the procedure described above.

2.10. Calculations and statistics

A stack with three images of emissions at 405 and 488 nm was recorded for each fish and organ. The ratio of emission at 405/488 of every individual measuring point was calculated and the mean of the three images in the stack was used as one datapoint (n).

The software Statistica (TIBCO software Inc.) was used for the statistical analyses. In the experiment describing ontogeny of the 405/488 ratio in embryos, data on 405/488 ratio in the cell disc from the 2-cell to the 50% epiboly stage was subjected to factorial repeated measurement ANOVA with zebrafish line (cyto, mito) and stage/time as design variables. Thereafter, the mito-line and then the cyto-line were subjected to the same analyses, only the design variables were organ and stage/time. Possible differences between organs were tested using one-way ANOVA at the different stages. In experiments where larvae were exposed to chemicals, data were subjected to nested ANOVA, individual fish nested in replicate dishes. Nonparametric tests were used when the data had inhomogenous variances. Differences and effects were considered significant at $p < 0.05$.

3. Results

The GSSG:GSH ratios measured via the roGFP probe were stable in muscles of larvae harboring the probe either in mitochondria (mito-line) or cytosol (cyto-line) for 60 min under the microscope with blanc incubations at 405 nm (GSSG):488 nm (GSH) ratios of 0.72 ± 0.01 and 0.16 ± 0.03 ($n = 3$), respectively (Fig. S1A). The reactivity of the probe was confirmed by H_2O_2 (oxidant) or DTT (reductant) treatments (Fig. S1B,C). H_2O_2 or DTT were added to microscope dishes with mito- or

cyto-larvae in increasing concentrations from 0 to 500 mM. The ratio in muscles of the mito-line increased upon addition of H_2O_2 from 0.75 ± 0.05 to 1.33 ± 0.22 and decreased in response to DTT from 0.78 ± 0.16 to 0.23 ± 0.02. In the cyto-line the ratio changed in response to increasing concentrations of H_2O_2 from 0.21 ± 0.04 to 1.18 ± 0.01 and to increasing concentrations of DTT from 0.24 ± 0.04 to 0.17 ± 0.01 (Fig.S1B). In addition to concentration-dependency, the probe also showed time-dependency in different areas of the larvae following the 405 nm:488 nm ratios in the mito-line for 60 min (Fig. S1C).The GSSG:GSH ratio in the muscle increased from 0.81 ± 0.13 to 1.46 ± 0.35 with H_2O_2 or decreased from 0.76 ± 0.03 to 0.22 ± 0.02 with DTT. Surprisingly, in the brain the GSSG:GSH ratio was almost unchanged upon H_2O_2 treatment. DTT decreased the ratio from 0.64 ± 0.11 to 0.18 ± 0.04.

3.1. The GSSG:GSH ratio in mitochondria and cytosol of developing zebrafish embryos

The different investigated stages of the zebrafish development are shown in Table 1 and partly in Fig. 1A. The 405:488 nm ratio of the Grx1-roGFP probe was measured between 0 and 50 h post fertilization (hpf, Fig. 1B,C). During the cleavage, blastula, and gastrula stages fluorescence was measured in the cell disk. In both the mito- and cyto-lines we observed a similar increase in the 405:488 nm ratio from the 2-cell stage until 50% epiboly from 0.40 ± 0.09 to 0.56 ± 0.04 ($p < 10^{-4}$) and 0.43 ± 0.1 to 0.56 ± 0.17 ($p < 10^{-4}$), respectively (Fig. 1B and C). Between 100% epiboly and after hatching, the GSSG:GSH ratio was stable in mitochondria in brain and muscle precursors (0.62 ± 0.03 and 0.64 ± 0.06, respectively), whereas it decreased in the cytosol of brain and muscle precursors as well as the tip of the tail, from 0.47 ± 0.02 to 0.29 ± 0.04 on average for the investigated organs ($p < 10^{-6}$, Fig. 1B and C). However, compared to the other organs, the cytosolic GSSG:GSH ratio was slightly higher at the tip of the tail during the stage "enhanced lengthening" (25 hpf, 0.49 ± 0.14 vs. 0.32 ± 0.05, $p = 0.02$) (Fig. 1C).

In addition, GSH and GSSG concentrations were measured chemically in whole embryos at 0, 11, 30, and 48 hpf. The results show that GSH concentrations were approximately 100 fold higher than GSSG concentrations throughout development (Fig. S2).

3.2. Effects of modulators of GSH metabolism and the toxicant PFOS on the GSSG:GSH ratio in muscles of zebrafish larvae after hatching

We tested whether different modulators of GSH with established or suggested clinical use affect the GSSG:GSH ratio in newly hatched larvae (50 hpf). N-acetyl-L-cysteine (NAC) is assumed to supply cysteine and

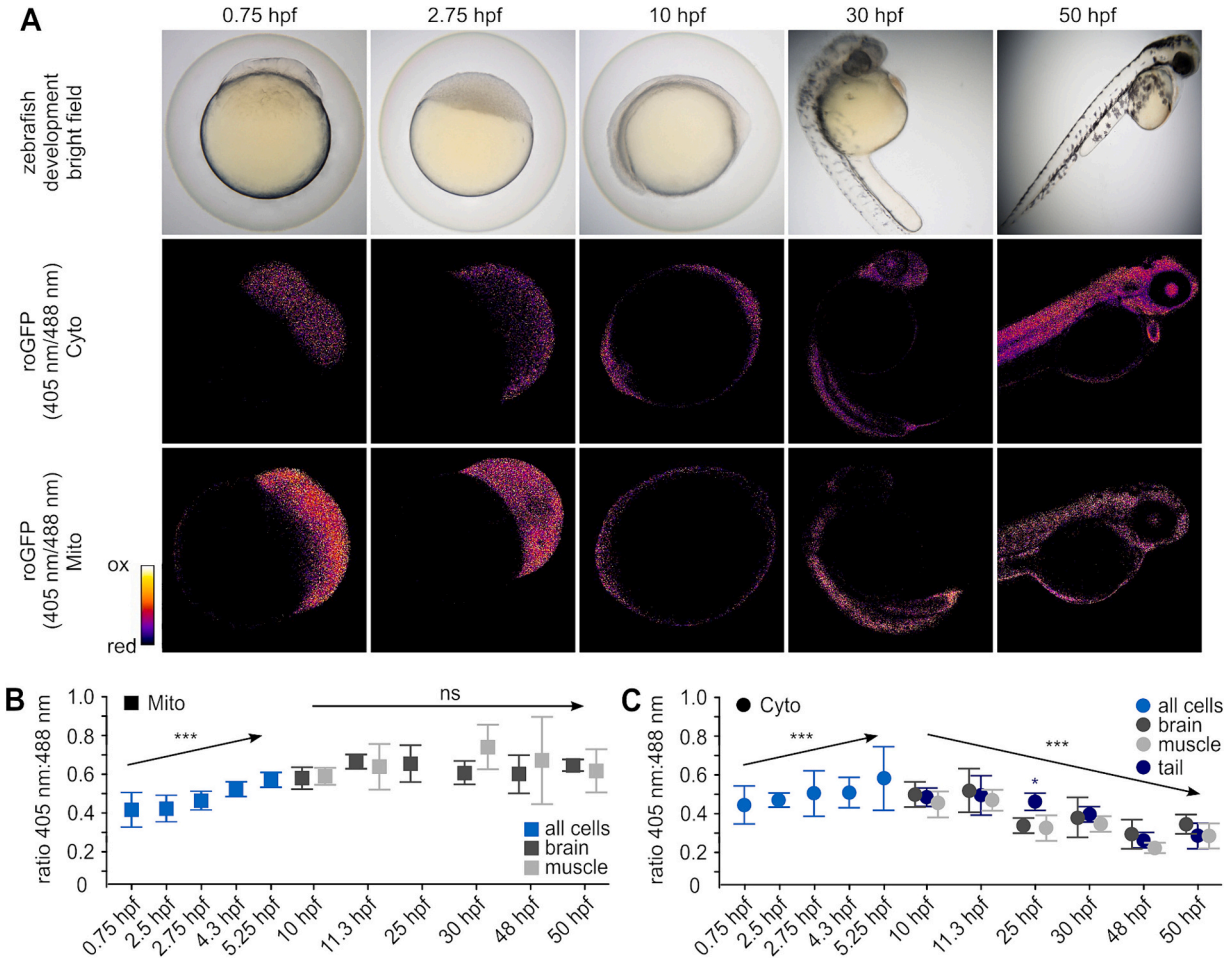

Fig. 1. The GSSG:GSH ratio in cytosol and mitochondria in the developing zebrafish is strictly regulated.
A) Bright field and ratiometric images of zebrafish harboring a mitochondrial (Mito) or a cytosolic localized Grx1-roGFP2 variant (Cyto) at indicated times after fertilization. Oxidized probe: excitation 405 nm, emission 510 nm, reduced probe: excitation 488 nm, emission 510 nm. B) The emission ratio of oxidized/reduced Grx1-roGFP signal was calculated for selected stages (see Tab. 1) and organs in mito- (B) and cyto- zebrafish lines (C) (mean ± SEM, four larvae per stage per experiment, 3 experiments, n=12). Arrows indicate the significance of repeated measurements ANOVA of the redox potential measured in the cell disc between the 2-cell stage and 50% epiboly, and from 100% epiboly until after hatching, in brain, muscle and tip of the tail (cyto-line only, C). Difference in redox potential between organs are shown with asterixes (one way ANOVA at single stages). * = $p < 0.05$, *** = $p < 0.001$.

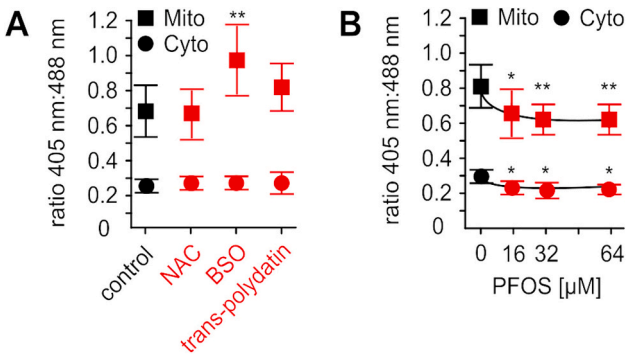

Fig. 2. Modulation of GSH metabolism at 50 hpf has only moderate impact on the GSSG:GSH ratio.
A) 405:488 nm ratios detected by the Grx1-roGFP probe in muscles of newly hatched zebrafish larvae, mito- and cyto-lines, after 24 hours of incubation with 250 µM N-acetyl-L-cysteine (NAC), 15 µM L-Buthionine-(S,R)-sulfoximine (BSO) or 40 µM trans-polydatin, mean ± SEM, three larvae per treatment per experiment, 3 experiments, n = 9, ** = $p < 0.01$. B) 405:488 nm ratios in muscles of newly hatched zebrafish larvae incubated for 24 hours with increasing concentrations of Perfluorooctane Sulfonate (PFOS), mean ± SEM, three larvae per treatment per experiment, 3 experiments, n = 9, * = $p < 0.05$, ** = $p < 0.01$.

thereby to increase GSH levels, since cysteine availability is rate limiting for GSH synthesis [33]. Cysteine arrives from either feed consumption, protein degradation, or through transsulfuration of homocysteine produced in the 1C metabolism [34–36]. NAC is generally used as dietary supplement, since it is more stable than cysteine [37]. Since >50 years, NAC is in clinical use against a variety of diseases in different organs including brain, lung, and liver [38]. After incubation of newly hatched larvae with NAC, the cytosolic and mitochondrial ratios were stable around 0.24 ± 0.03 and 0.61 ± 0.13, respectively (Fig. 2A). Buthionine sulphoximine (BSO) enhances the therapeutic effect of several anti-cancer drugs in cells resistant by increased GSH levels (e.g. [39]). BSO inhibits γ-glutamylcysteine synthetase, the rate limiting enzyme of GSH synthesis [40]. BSO did not change the GSSG:GSH ratio in the cytosol but led to a more oxidized ratio in mitochondria compared to control (0.88 ± 0.19 vs. 0.62 ± 0.13, $p = 0.007$, Fig. 2A). *trans*-Polydatin, the 3-β-D-glucoside of resveratrol, decreased endiometriosis-related pain in small patient samples [41] and is discussed as promising therapeutic strategy against metabolic diseases such as atherosclerosis, diabetes, or non-alcoholic steatohepatitis [42]. This compound blocks the penthose phosphate cycle and therefore limits the production of NADPH, inhibiting several redox reactions, including reduction of GSSG by GSH reductase [43], but did also not affect cytosolic or mitochondrial GSSG:GSH ratios (Fig. 2A).

Incubation with 16, 32, and 64 µM PFOS modulated both cytosolic and mitochondrial GSSG:GSH ratios in zebrafish larvae (Fig. 2B). In the mitochondria, the ratio decreased anti-parallel to PFOS concentrations from 0.82 ± 0.11 to 0.62 ± 0.09 ($p < 0.03$), whereas the ratio in the cytosol dropped from 0.29 ± 0.04 to 0.23 ± 0.04 ($p < 0.01$) already at 16 µM PFOS and remained constant.

All above mentioned measurements were performed after 24 h of treatment with the respecive compounds.

3.3. Early modulation of GSH metabolism by carmustine leads to malformation and death of zebrafish embryos

Newly fertilized eggs/embryos were incubated with 200 µM carmustine for 10 h. Whereas the 405:488 nm ratio increased moderately in mitochondria of control fish between 1 hpf (0.68 ± 0.06) and 10 hpf (0.77 ± 0.06), carmustine treatment increased the ratio significantly from 0.68 ± 0.06 to 1.01 ± 0.09 ($p < 10^{-5}$) (Fig. 3A and B). In the

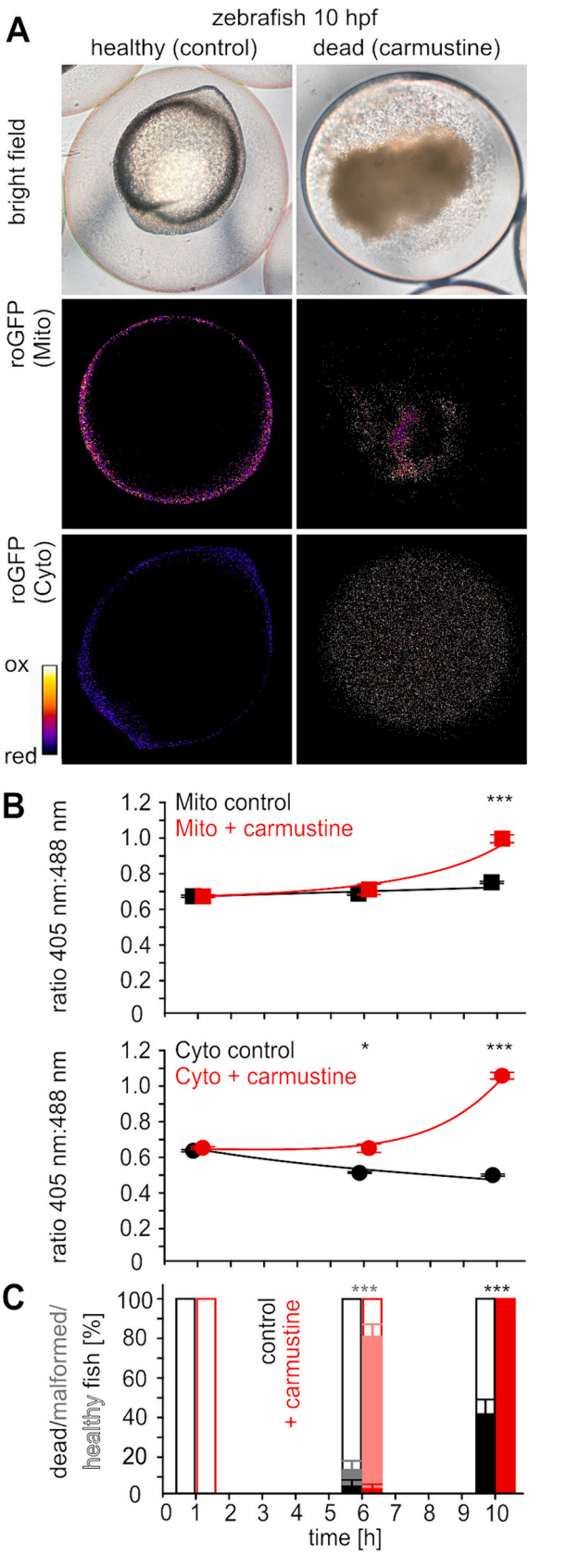

(caption on next page)

Fig. 3. Disturbed GSSG:GSH ratio affect proper zebrafish ontogeny.
A) Bright field and ratiometric (based on oxidized (excitation 405 nm, emission 510 nm) and reduced Grx1- roGFP2 (excitation 488 nm, emission 510 nm)) images of zebrafish embryos harboring a mitochondrial (Mito) or a cytosolic localized Grx1-roGFP2 variant (Cyto) 10 hpf with and without treatment with 200 μM carmustine. B) The emission ratio of oxidized/reduced Grx1-roGFP signal was calculated for zebrafish with and without carmustine treatment at 1, 6, and 10 hpf in Mito and Cyto embryos, mean of all fish with an emission signal > 100 ± SD, 3 experiments, n = 7-16, * = $p < 0.05$, *** = $p < 0.001$. C) All zebrafish of the three independent experiments were checked for malformation or death. The percentage of healhty, malformed, and dead embryos are shown for all carmustine-treated (red) and untreated zebrafish (Mito and Cyto, black) at 1, 6, and 10 hpf, mean ± SD, 3 experiments, n = 232-449, *** = $p < 0.001$.

cytosol of control embryos the ratio changed from 0.63 ± 0.08 to 0.5 ± 0.07 (Fig. 3A and B). In presence of carmustine the ratio increased from 0.65 ± 0.1 to 1.07 ± 0.11 at 10 hpf ($p \langle 10^{-10}$) (Fig. 3A and B). At this time point nearly all zebrafish embryos (99.47%) were already dead (compared to 43.37 ± 6.1% in control embryos, $p < 10^{-9}$, Fig. 3A and C). The slight increase in the GSSG:GSH ratio after 6 hpf (0.64 ± 0.16 vs. 0.51 ± 0.04 in cytosol ($p < 0.03$) and 0.71 ± 0.14 vs. 0.69 ± 0.07 in mitochondria, Fig. 3B) induced malformation (arrest of cell division and development) in 81.58 ± 4.9% of carmustine treated zebrafish compared to 8.95 ± 6.07% in control fish ($p < 10^{-9}$, Fig. 3C).

4. Discussion

With this study we investigated whether the GSSG:GSH ratio is strictly regulated during embryonic development and the importance of this regulation using zebrafish, the most prominent vertebrate model for this process. Therefore, we followed the GSSG:GSH ratio in different organelles and organs during development and manipulated the GSH metabolism with various compounds at different time points. The GSSG:GSH ratio represents the most abundant cellular redox circuit. Therefore, the GSH-dependent reduction potential (E_{hGSH}) is thought to determine biological processes [44]. As several times before [7,45] this view is questioned by this study. A reducing E_{hGSH} seems to be important for cell survival and function but specific processes do not depend on the overall redox state. Because of the low abundance of GSSG compared to GSH, just some molecules of GSSG are able to heavily change the E_{hGSH} [46]. Fig. S2 shows that also during different stages of zebrafish development the concentration of GSSG is quite low. Spatiotemporal enzymatic activities regulating redox signaling events essential for proper embryonic development may not depend directly or exclusively on the cellular E_{hGSH} but on local changes or indirectly via specific modifications such as S-glutathionylation or S-nitrosation by nitrosoglutathione [47]. To follow the GSSG:GSH ratio we confirmed that the Grx1-roGFP2 probe works in mitochondria and the cytosol in brain and muscles (Fig. S1). In contrast to muscles and DTT, the probe in the brain did react on H_2O_2 treatment only with small changes in the GSSG:GSH ratio although external H_2O_2 reaches the zebrafish brain [48]. It was shown that superoxide dismutase as well as catalase activity was stronger upregulated in the brain than in other organs of adult zebrafish upon H_2O_2 formation inducing treatments [49], however, if these findings are related to ours needs further research. Without treatment, different organs had largely similar GSSG:GSH ratios in both mitochondria and cytosol indicating that the enzymes controlling the organellar E_{hGSH} of zebrafish embryos and yolk sac larvae are centrally regulated similar to the master clock regulating all organellar circadian rhythm systems [50]. Nevertheless, our study revealed an exception with a more pronounced shift to cytosolic GSSG compared to other organs in the tip of the tail at the enhanced lengthening stage. Since this stage is characterized by tail growth, the higher GSSG:GSH ratio is in agreement with findings demonstrating that cell growth is accompanied by a more oxidized intracellular environment [51]. Moreover, increasing growth coincides with more oxidized tissue E_{hGSH} in both Atlantic cod and Atlantic salmon [20–23].

As described before, the average E_{hGSH} in whole zebrafish during embryogenesis is reduced at fertilization, reaches a peak of oxidation at the gastrula stage and is gradually reduced during organogenesis, reaching a similar level at hatching as at fertilization [15,16]. Assuming that the cytosol represents a relatively large fraction of the cell, this is in line with our present study where the cytosolic GSSG:GSH ratio increased between fertilization and gastrulation and then decreased between gastrulation and hatching.

Transient elevation of H_2O_2 concentration is involved in processes such as regeneration, wound healing, growth of peripheral sensory axons and enhancing cell plasticity [25,52]. In embryogenesis of zebrafish, H_2O_2 concentrations measured by the ratiometric probe HyPer showed a highly spatiotemporal variation, with average whole-body concentrations increasing from fertilization until the 20-somite stage. The concentrations stayed high until hatching (48 hpf) but decreased afterwards to a level at 72 hpf approximately 4-fold lower than that at hatching [25]. As suggested by the presented data, the measured GSSG:GSH ratios might reflect the capacity to adapt to these H_2O_2 concentrations. The adaption capacity seems to be higher in cytosol than in mitochondria and in differentiated neurons than in stem cells as shown with pluripotent mouse embryonal cells (P19) [53]. Based on that publication, early embryonic stages are not as efficient as later stages in facing increasing H_2O_2 levels. In line, the GSSG:GSH ratio becomes more oxidized upon increasing H_2O_2 levels within the first 5–6 hpf in both cytosol and mitochondria (Fig. 1B,C). Whith the growing number of differentiated cells, the higher adaption ability in the cytosol might lead to a re-reduction of the GSSG:GSH ratio, whereas mitochondria keep it at least constant. To study further the ability to keep E_{hGSH} constant under stress conditions, newly hatched larvae were exposed to modulators of the GSH metabolism, namely NAC, BSO, or trans-polydatine, (Fig. 2A). NAC showed no influence on the GSSG:GSH ratio in mitochondria and cytosol of muscles indicating that our data resemble the results in mammals and patients showing that NAC increases GSH levels only under conditions of GSH deficiency (summarized in [54]). As indicated by the here provided data and earlier studies, fish share obviously an effective negative feedback regulation with higher vertebrates [24]. Moreover, NAC functions are not always connected to the formation of elevated GSH levels. A new mechanism suggests that instead of elevated GSH levels, the increased formation of H_2S and sulfane sulfur are responsible for the protective functions of NAC [55]. These sulfur species should be checked in NAC-treated zebrafish as well.

BSO did not change the GSSG:GSH ratio in the cytosol but led to a more oxidized ratio in mitochondria compared to control. This result could be explained by the finding that in contrast to the cytosol, mitochondria are not able to export GSSG [56]. Under conditions of decreased levels of total GSH, the remaining GSSG could increase the GSSG:GSH ratio. Moreover, as described before, mitochondria adapt not as good as the cytosol to oxidation. The treatment with 40 μM trans-polydatin did also not affect cytosolic or mitochondrial GSSG:GSH ratios, although lower concentrations between 10 and 20 μM showed effects in zebrafish such as protection against EtOH [57]. *trans*-Polydatin is suggested to affect GSH concentrations via diminished NADPH levels. Unfortunately, there is no direct proof for this mechanism in zebrafish. However, the finding that trans-polydatin inhibits formation of zebrafish vasculature [58], a pentose phosphate pathway-dependent process [59], provides indirect evidence for this mode of action. A direct proof is now possible by the recently established zebrafish line harboring the NADPH sensor NERNST [60]. Of course the limited effects of these three modulators might be also related to the time point and the time span of treatment. NAC, BSO, and trans-polydatin, were doubted to pass through the chorion, therefore, these treatments were done for 24 h after hatching when many developmental processes were already finished and the zebrafish had time to compensate potential changes in the GSSG:GSH ratio. Zebrafish larvae exposed to tert-Butyl hydroperoxide or yeast cells treated with H_2O_2 become more oxidized during the first 10 min,

but the E_{hGSH} was already restored after 30 min [46,61], representing a fast adaption to the changed conditions. Therefore, we tested the importance of strict control of the E_{hGSH} during embryogenesis by incubation of newly fertilized eggs with carmustine, an inhibitor of GSH reductase. The measured 405:488 nm ratio increased over time and led to malformed and dead embryos.

In addition, we tested whether environmental pollution impacts the E_{hGSH}. PFOS is a persistent environmental contaminant and is one of the most dominant chemical forms of the group of *per*- and polyfluoroalkyl substances (PFAS), which have been used in many different industrial applications such as fire extinguishing foam or Teflon. PFOS exposure has recently been risk assessed for humans [62] and maximum levels have been set for food products, including seafood [63]. It was previously shown that PFOS induce oxidative damage in zebrafish embryos [29,64]. Incubation with PFOS lowered both cytosolic and mitochondrial GSSG:GSH ratios in zebrafish larvae after 24 h of treatment. This indicates that we see only the result of over compensation of the oxidative challenge induced by PFOS. Previous results have indicated that increased production of oxidants stimulates GSH synthesis leading to a lowered E_{hGSH}, a protective mechanism that has been indicated in several other studies [21,23]. Studies on molecular mechanisms of PFOS showed an activation of the NrF2 signaling, leading to an upregulation of the antioxidative response [65]. The NrF2 mediation of the GSH redox system plays a mitigating role in PFOS embryonic responses through NrF2 and PPAR nuclear factor cross talking [66]. Therefore, it is tempting to speculate that PFOS-induced oxidative challenge might activate the GSH antioxidant response to combat oxidative damage.

The provided data clearly confirm that disturbances of the GSSG:GSH ratio affect proper ontogeny. The GSSG:GSH ratio seems to follow/compensate the H_2O_2 levels that drives the differentiation program. Thereby, oxidative damage is prevented which leads otherwise to malformation or even death. However, not only an increased/oxidized ratio, but also a decreased/reduced ratio which leads to reductive stress, affect embryogenesis as shown for mammals [67]. Therefore, PFOS or other environmental pollutants disturbing the E_{hGSH} are a risk for proper development of embryos of zebrafish and other vertebrates.

5. Conclusion

In summary, the E_{hGSH} of different cells and organs may be strictly and centrally regulated, since brain and muscle had similar GSSG:GSH ratios in mitochondria and cytosol throughout zebrafish embryogenesis. Modulation of the GSSG:GSH ratio during embryogenesis leads to malformation and death. The environmental pollutant PFOS changed the GSSG:GSH ratio and could thereby affect proper development.

Funding

The study was funded by the Norwegian Ministry of Trade, Industry and Fisheries; IMR-project 15468 Vekst og ROS and the Deutsche Forschungsgemeinschaft (DFG, German Research Foundation) - 417677437/GRK2578. Wuxiao Zang and Peng Yin were visiting scientists with grants from the China Scholarship Council, China. Open access was provided via the DEAL project.

CRediT authorship contribution statement

Kristin Hamre: Conceptualization, Data curation, Formal analysis, Funding acquisition, Investigation, Methodology, Project administration, Supervision, Validation, Writing – original draft, Writing – review & editing. **Wuxiao Zhang:** Investigation, Methodology, Writing – review & editing. **Maren Hoff Austgulen:** Investigation, Methodology, Supervision, Validation, Writing – review & editing. **Eva Mykkeltvedt:** Investigation, Methodology, Supervision, Validation, Writing – review & editing. **Peng Yin:** Investigation, Methodology, Validation, Writing – review & editing. **Marc Berntssen:** Conceptualization, Investigation, Validation, Writing – original draft. **Marit Espe:** Conceptualization, Investigation, Validation, Writing – original draft. **Carsten Berndt:** Conceptualization, Investigation, Methodology, Resources, Software, Visualization, Writing – original draft.

Declaration of competing interest

No competing interest declared.

Data availability

All relevant data can be found within the manuscript and its supplementary information.

Acknowledgements

At IMR, Bergen, Norway, Ståle Ellingsen and Øystein Sæle helped with the confocal microscope, Bjørnar Skjold and Arna Kazizic took care of the zebrafish facility and fish husbandry. Leticia Prates Roma (Homburg, Germany) helped with the protocol to generate ratiometric pictures.

Appendix A. Supplementary data

Supplementary data to this article can be found online at https://doi.org/10.1016/j.bbagen.2024.130603.

References

[1] H. Sies, C. Berndt, D.P. Jones, Oxidative Stress, in: R.D. Kornberg (Ed.), Annual Review of Biochemistry, Vol 86 vol. 86, 2017, pp. 715–748.
[2] H. Sies, Oxidative eustress and oxidative distress, Free Radic. Biol. Med. 165 (2021).
[3] C. Berndt, C.H. Lillig, Redox regulation of differentiation and de-differentiation, BBA-Gen. Subjects 2015 (1850) 1467–1468.
[4] J.M. Hansen, C. Harris, Glutathione during embryonic development, BBA-Gen. Subjects 2015 (1850) 1527–1542.
[5] J.M. Hansen, D.P. Jones, C. Harris, The redox theory of development, Antioxid. Redox Signal. 32 (2020) 715–740.
[6] H. Sies, D.P. Jones, Reactive oxygen species (ROS) as pleiotropic physiological signalling agents, Nat. Rev. Mol. Cell Biol. 21 (2020) 363–383.
[7] C. Berndt, C.H. Lillig, L. Flohé, Redox regulation by glutathione needs enzymes, Front. Pharmacol. 5 (2014).
[8] D.P. Jones, H. Sies, The redox code, Antioxid. Redox Signal. 23 (2015) 734–746.
[9] E.M. Hanschmann, J.R. Godoy, C. Berndt, C. Hudemann, C.H. Lillig, Thioredoxins, Glutaredoxins, and Peroxiredoxins-molecular mechanisms and health significance: from cofactors to antioxidants to redox signaling, Antioxid. Redox Signal. 19 (2013) 1539–1605.
[10] C.H. Lillig, C. Berndt, Glutaredoxins in thiol/disulfide exchange, Antioxid. Redox Signal. 18 (2013) 1654–1665.
[11] Y.M. Go, D.P. Jones, The redox proteome, J. Biol. Chem. 288 (2013) 26512–26520.
[12] D.P. Jones, Redox potential of GSH/GSSG couple: Assay and biological significance, in: H. Sies, L. Packer (Eds.), Protein Sensors and Reactive Oxygen Species, Pt B, Thiol Enzymes and Proteins vol. 348, 2002, pp. 93–112.
[13] L. Bräutigam, C. Berndt, Redox regulation during zebrafish development, in: C. Berndt, C.H. Lillig (Eds.), Redox Regulation of Differentiation and de-Differentiation, CRC Press, Boca Raton, London, New York, 2022, pp. 57–68.
[14] O. Breus, T. Dickmeis, Genetically encoded thiol redox-sensors in the zebrafish model: lessons for embryonic development and regeneration, Biol. Chem. 402 (2021) 363–378.
[15] A.R. Timme-Laragy, J.V. Goldstone, B.R. Imhoff, J.J. Stegeman, M.E. Hahn, J. M. Hansen, Glutathione redox dynamics and expression of glutathione-related genes in the developing embryo, Free Radic. Biol. Med. 65 (2013) 89–101.
[16] A.R. Timme-Laragy, M.E. Hahn, J.M. Hansen, A. Rastogi, M.A. Roy, Redox stress and signaling during vertebrate embryonic development: regulation and responses, Semin. Cell Dev. Biol. 80 (2018) 17–28.
[17] L. Bräutigam, L.D.E. Jensen, G. Poschmann, S. Nyström, S. Bannenberg, K. Dreij, K. Lepka, T. Prozorovski, S.J. Montano, O. Aktas, P. Uhlén, K. Stühler, Y.H. Cao, A. Holmgren, C. Berndt, Glutaredoxin regulates vascular development by reversible glutathionylation of sirtuin 1, Proc. Natl. Acad. Sci. USA 110 (2013) 20057–20062.
[18] L. Bräutigam, L.D. Schütte, J.R. Godoy, T. Prozorovski, M. Gellert, G. Hauptmann, A. Holmgren, C.H. Lillig, C. Berndt, Vertebrate-specific glutaredoxin is essential for brain development, Proc. Natl. Acad. Sci. USA 108 (2011) 20532–20537.
[19] C. Wilms, K. Lepka, F. Häberlein, S. Edwards, J. Felsberg, L. Pudelko, T. T. Lindenberg, G. Poschmann, N. Qin, K. Volbracht, T. Prozorovski, S.G. Meuth, U. D. Kahlert, M. Remke, O. Aktas, G. Reifenberger, L. Bräutigam, B. Odermatt,

C. Berndt, Glutaredoxin 2 promotes SP-1-dependent CSPG4 transcription and migration of wound healing NG2 glia and glioma cells: enzymatic Taoism, Redox Biol. 49 (2022).
[20] S. Penglase, R.B. Edvardsen, T. Furmanek, I. Ronnestad, O. Karlsen, T. van der Meeren, K. Hamre, Diet affects the redox system in developing Atlantic cod (Gadus morhua) larvae, Redox Biol. 5 (2015) 308–318.
[21] K. Hamre, G. Micallef, M. Hillestad, J. Johansen, S. Remo, W.X. Zhang, E. Odegård, P. Araujo, A.J.P. Philip, R. Waagbo, Changes in daylength and temperature from April until august for Atlantic salmon (Salmo salar) reared in sea cages, increase growth, and may cause consumption of antioxidants, onset of cataracts and increased oxidation of fillet astaxanthin, Aquaculture 551 (2022).
[22] P. Yin, T. Saito, P.G. Fjelldal, B.T. Björnsson, S.C. Remo, T.J. Hansen, S. Sharma, R. E. Olsen, K. Hamre, Seasonal changes in photoperiod: effects on growth and redox signaling patterns in Atlantic Salmon Postsmolts, Antioxidants 12 (2023).
[23] P. Yin, B.T. Björnsson, P.G. Fjelldal, T. Saito, S.C. Remo, R.B. Edvardsen, T. Hansen, S. Sharma, R.E. Olsen, K. Hamre, Impact of antioxidant feed and growth manipulation on the redox regulation of Atlantic Salmon Smolts, Antioxidants 11 (2022).
[24] K. Hamre, B.E. Torstensen, A. Maage, R. Waagbo, R.K. Berge, S. Albrektsen, Effects of dietary lipid, vitamins and minerals on total amounts and redox status of glutathione and ubiquinone in tissues of Atlantic salmon (Salmo salar): a multivariate approach, Br. J. Nutr. 104 (2010) 980–988.
[25] C. Gauron, F. Meda, E. Dupont, S. Albadri, N. Quenech'Du, E. Ipendey, M. Volovitch, F. Del Bene, A. Joliot, C. Rampon, S. Vriz, Hydrogen peroxide (H₂O₂) controls axon pathfinding during zebrafish development, Dev. Biol. 414 (2016) 133–141.
[26] C. Rampon, M. Volovitch, A. Joliot, S. Vriz, Hydrogen peroxide and redox regulation of developments, Antioxidants 7 (2018).
[27] L. Bräutigam, L. Pudelko, A.S. Jemth, H. Gad, M. Narwal, R. Gustafsson, S. Karsten, J.C. Puigvert, E. Homan, C. Berndt, U.W. Berglund, P. Stenmark, T. Helleday, Hypoxic signaling and the cellular redox tumor environment determine sensitivity to MTH1 inhibition, Cancer Res. 76 (2016) 2366–2375.
[28] M. Gutscher, A.L. Pauleau, L. Marty, T. Brach, G.H. Wabnitz, Y. Samstag, A. J. Meyer, T.P. Dick, Real-time imaging of the intracellular glutathione redox potential, Nat. Methods 5 (2008) 553–559.
[29] J. Huang, Q.Y. Wang, S. Liu, M. Zhang, Y. Liu, L.W. Sun, Y.M. Wu, W.Q. Tu, Crosstalk between histological alterations, oxidative stress and immune aberrations of the emerging PFOS alternative OBS in developing zebrafish, Sci. Total Environ. 774 (2021).
[30] C.B. Kimmel, W.W. Ballard, S.R. Kimmel, B. Ullmann, T.F. Schilling, STAGES OF EMBRYONIC-DEVELOPMENT OF THE ZEBRAFISH, Dev. Dyn. 203 (1995) 253–310.
[31] Y. Fujikawa, L.P. Roma, M.C. Sobotta, A.J. Rose, M.B. Diaz, G. Locatelli, M. O. Breckwoldt, T. Misgeld, M. Kerschensteiner, S. Herzig, K. Müller-Decker, T. P. Dick, Mouse redox histology using genetically encoded probes, Sci. Signal. 9 (2016).
[32] K.E. Sant, H.M. Jacobs, K.A. Borofski, J.B. Moss, A.R. Timme-Laragy, Embryonic exposures to perfluorooctanesulfonic acid (PFOS) disrupt pancreatic organogenesis in the zebrafish, Danio rerio, Environ. Pollut. 220 (2017) 807–817.
[33] M.E. Anderson, A. Meister, Transport and direct utilization of gamma-GLUTAMYLCYST(e)INE for glutathione synthesis, Proceedings of the National Academy of Sciences of the United States of America-Biological Sciences 80 (1983) 707–711.
[34] M. Espe, K.H. Skjærven, M. Chen, V. Vikeså, A.C. Adam, T. Saito, E. Holen, The level of 1C diets fed prior to cell isolation affects lipid metabolism in primary liver cells isolated from Atlantic salmon (Salmo salar), Aquac. Nutr. 26 (2020) 1019–1025.
[35] M. Espe, V. Vikeså, T.H. Thomsen, A.C. Adam, T. Saito, K.H. Skjærven, Atlantic salmon fed a nutrient package of surplus methionine, vitamin B12, folic acid and vitamin B6 improved growth and reduced the relative liver size, but when in excess growth reduced, Aquac. Nutr. 26 (2020) 477–489.
[36] G. Morris, G. Anderson, O. Dean, M. Berk, P. Galecki, M. Martin-Subero, M. Maes, The glutathione system: a new drug target in Neuroimmune disorders, Mol. Neurobiol. 50 (2014) 1059–1084.
[37] F.J. Zhang, S.S. Lau, T.J. Monks, The Cytoprotective effect of N-acetyl-L-cysteine against ROS-induced cytotoxicity is independent of its ability to enhance glutathione synthesis, Toxicol. Sci. 120 (2011) 87–97.
[38] G.K. Schwalfenberg, N-acetylcysteine: a review of clinical usefulness (an old drug with new tricks), J. Nutrit. and Metab. 2021 (2021).
[39] J.G. Villablanca, S.L. Volchenboum, H. Cho, M.H. Kang, S.L. Cohn, C.P. Anderson, A. Marachelian, S. Groshen, D. Tsao-Wei, K.K. Matthay, J.M. Maris, C. E. Hasenauer, S. Czarnecki, H. Lai, F. Goodarzian, H. Shimada, C.P. Reynolds, A phase I new approaches to neuroblastoma therapy study of Buthionine Sulfoximine and Melphalan with autologous stem cells for recurrent/refractory high-risk neuroblastoma, Pediatr. Blood Cancer 63 (2016) 1349–1356.
[40] A. Tagde, H. Singh, M.H. Kang, C.P. Reynolds, The glutathione synthesis inhibitor buthionine sulfoximine synergistically enhanced melphalan activity against preclinical models of multiple myeloma, Blood Cancer J. 4 (2014).
[41] U. Indraccolo, S.R. Indraccolo, F. Mignini, Micronized palmitoylethanolamide/trans−polydatin treatment of endometriosis-related pain: a meta-analysis, Ann. Ist. Super. Sanita 53 (2017) 125–134.
[42] J.L. Luo, S. Chen, L. Wang, X.H. Zhao, C.L. Piao, Pharmacological effects of polydatin in the treatment of metabolic diseases: a review, Phytomedicine 102 (2022).
[43] L. Mele, F. Paino, F. Papaccio, T. Regad, D. Boocock, P. Stiuso, A. Lombardi, D. Liccardo, G. Aquino, A. Barbieri, C. Arra, C. Coveney, M. La Noce, G. Papaccio, M. Caraglia, V. Tirino, V. Desiderio, A new inhibitor of glucose-6-phosphate dehydrogenase blocks pentose phosphate pathway and suppresses malignant proliferation and metastasis in vivo, Cell Death Dis. 9 (2018).
[44] F.Q. Schafer, G.R. Buettner, Redox environment of the cell as viewed through the redox state of the glutathione disulfide/glutathione couple, Free Radic. Biol. Med. 30 (2001) 1191–1212.
[45] L. Flohé, The fairytale of the GSSG/GSH redox potential, BBA-Gen. Subjects 2013 (1830) 3139–3142.
[46] B. Morgan, D. Ezerina, T.N.E. Amoako, J. Riemer, M. Seedorf, T.P. Dick, Multiple glutathione disulfide removal pathways mediate cytosolic redox homeostasis, Nat. Chem. Biol. 9 (2013) 119–125.
[47] H.Q. Zhang, H.J. Forman, Glutathione synthesis and its role in redox signaling, Semin. Cell Dev. Biol. 23 (2012) 722–728.
[48] D. Engur, C. Ercan, K.U. Kiser, S. Tufekci, S.C. Soy, G. Micili, S. Ozhan, A. Guven, S. Kumral, Genc, hydrogen peroxide signaling modulates neuronal differentiation via microglial polarization and Wnt/β- catenin pathway, Eur. Rev. Med. Pharmacol. Sci. 27 (2023) 5083–5096.
[49] A.P.D. Araújo, T.M. da Luz, T.L. Rocha, M.A.I. Ahmed, D.D.E. Silva, M.M. Rahman, G. Malafaia, Toxicity evaluation of the combination of emerging pollutants with polyethylene microplastics in zebrafish: perspective study of genotoxicity, mutagenicity, and redox unbalance, J. Hazard. Mater. 432 (2022).
[50] X. Yu, N.P. Franks, W. Wisden, Brain Clocks, Sleep, and Mood, in: O. Engmann, M. Brancaccio (Eds.), Circadian Clock in Brain Health and Disease vol. 1344, 2021, pp. 71–86.
[51] A. Corcoran, T.G. Cotter, Redox regulation of protein kinases, FEBS J. 280 (2013) 1944–1965.
[52] C. Berndt, C. Wilms, M. Thauvin, S. Vriz, Redox-Regulated Brain Development, in: H. Sies (Ed.), Oxidative Stress: Eustress and Distress, Elsevier, 2020.
[53] B.M. Davies, J.K. Katayama, J.E. Monsivais, J.R. Adams, M.E. Dilts, A.L. Eberting, J.M. Hansen, Real-time analysis of dynamic compartmentalized GSH redox shifts and H2O2 availability in undifferentiated and differentiated cells, BBA-Gen. Subjects 1867 (2023).
[54] B. Pedre, U. Barayeu, D. Ezerina, T.P. Dick, The mechanism of action of N-acetylcysteine (NAC): the emerging role of H₂S and sulfane sulfur species, Pharmacol. Ther. 228 (2021).
[55] D. Ezerina, Y. Takano, K. Hanaoka, Y. Urano, T.P. Dick, N-Acetyl Cysteine Functions as a Fast-Acting Antioxidant by Triggering Intracellular H₂S and Sulfane Sulfur Production, Cell Chem. Biol. 25 (2018) 447-+.
[56] K. Olafsdottir, D.J. Reed, Retention of oxidized glutathione by isolated rat-liver mitochondria during hydroperoxide treatment, Biochim. Biophys. Acta 964 (1988) 377–382.
[57] Y.L. Lai, C.Y. Zhou, P. Huang, Z.Y. Dong, C. Mo, L.P. Xie, H.Y. Lin, Z.T. Zhou, G. H. Deng, Y. Liu, Y.Y. Chen, S.H. Huang, Z.Y. Wu, X.G. Sun, L. Gao, Z.P. Lv, Polydatin alleviated alcoholic liver injury in zebrafish larvae through ameliorating lipid metabolism and oxidative stress, J. Pharmacol. Sci. 138 (2018) 46–53.
[58] W.H. Hu, H.Y. Wang, X.P. Kong, Q.P. Xiong, K.K.M. Poon, L. Xu, R. Duan, G.K. L. Chan, T.T.X. Dong, K.W.K. Tsim, Polydatin suppresses VEGF-induced angiogenesis through binding with VEGF and inhibiting its receptor signaling, FASEB J. 33 (2019) 532–544.
[59] N. Facchinello, M. Astone, M. Audano, R.E. Oberkersch, M. Spizzotin, E. Calura, M. Marques, M. Crisan, N. Mitro, M.M. Santoro, Oxidative pentose phosphate pathway controls vascular mural cell coverage by regulating extracellular matrix composition, nature, Metabolism 4 (2022) 123-+.
[60] P.E. Molinari, A.R. Krapp, A. Weiner, H.M. Beyer, A.K. Kondadi, T. Blomeier, M. López, P. Bustos-Sanmamed, E. Tevere, W. Weber, A.S. Reichert, N. B. Calcaterra, M. Beller, N. Carrillo, M.D. Zurbriggen, NERNST: a genetically-encoded ratiometric non-destructive sensing tool to estimate NADP(H) redox status in bacterial, plant and animal systems, Nat. Commun. 14 (2023).
[61] A. Rastogi, C.W. Clark, S.M. Conlin, S.E. Brown, A.R. Timme-Laragy, Mapping glutathione utilization in the developing zebrafish (Danio rerio) embryo, Redox Biol. 26 (2019).
[62] D. Schrenk, M. Bignami, L. Bodin, J.K. Chipman, J. del Mazo, B. Grasl-Kraupp, C. Hogstrand, L. Hoogenboom, J.C. Leblanc, C.S. Nebbia, E. Nielsen, E. Ntzani, A. Petersen, S. Sand, C. Vleminckx, H. Wallace, L. Barregård, S. Ceccatelli, J. P. Cravedi, T.I. Halldorsson, L.S. Haug, N. Johansson, H.K. Knutsen, M. Rose, A. C. Roudot, H. Van Loveren, G. Vollmer, K. Mackay, F. Riolo, T. Schwerdtle, E.P.C. F. Chain, Risk to human health related to the presence of perfluoroalkyl substances in food, EFSA J. 18 (2020).
[63] EC, COMMISSION REGULATION (EU) 2022/2388 of 7 December 2022 amending Regulation (EC) No 1881/2006 as regards maximum levels of perfluoroalkyl substances in certain foodstuffs official Journal of the Europian Union, L316/38, 2022.
[64] X.J. Shi, Y.B. Du, P.K.S. Lam, R.S.S. Wu, B.S. Zhou, Developmental toxicity and alteration of gene expression in zebrafish embryos exposed to PFOS, Toxicol. Appl. Pharmacol. 230 (2008) 23–32.
[65] J.L. Xu, P. Shimpi, L. Armstrong, D. Salter, A.L. Slitt, PFOS induces adipogenesis and glucose uptake in association with activation of Nrf2 signaling pathway, Toxicol. Appl. Pharmacol. 290 (2016) 21–30.
[66] K.E. Sant, P.P. Sinno, H.M. Jacobs, A.R. Timme-Laragy, Nrf2a modulates the embryonic antioxidant response to perfluorooctanesulfonic acid (PFOS) in the zebrafish, Danio rerio, Aquat. Toxicol. 198 (2018) 92–102.
[67] M.S. Sharpley, F.T. Chi, J. ten Hoeve, U. Banerjee, Metabolic plasticity drives development during mammalian embryogenesis, Dev. Cell 56 (2021) 2329-+.